Ecotoxicology and Environmental Safety 220 (2021) 112345

Contents lists available at ScienceDirect

Ecotoxicology and Environmental Safety

journal homepage: www.elsevier.com/locate/ecoenv

Effects of microplastics (MPs) and tributyltin (TBT) alone and in combination on bile acids and gut microbiota crosstalk in mice

Ping Jiang [a,b,1], Ge-hui Yuan [a,1], Bao-rong Jiang [a], Jing-yi Zhang [a], Yu-qian Wang [a], Hui-jie Lv [a], Zhan Zhang [a,b], Jia-lin Wu [a], Qian Wu [a,b], Lei Li [a,b,*]

[a] Center for Global Health, School of Public Health, Nanjing Medical University, 101 Longmian Avenue, Nanjing, Jiangsu 211166, PR China
[b] Key Lab of Modern Toxicology of Ministry of Education, School of Public Health, Nanjing Medical University, 101 Longmian Avenue, Nanjing, Jiangsu 211166, PR China

ARTICLE INFO

Edited by Professor Bing Yan

Keywords:
Microplastics
Tributyltin
Bile acids
Gut microbiome
Dysbiosis

ABSTRACT

Microplastics (MPs) and tributyltin (TBT) are both potential environmental pollutants that enter organisms through the food chain and affect bodily functions. However, the effects and mechanisms of MPs and TBT exposure (especially the co-exposure of both pollutants) on mammals remain unclear. In this study, Φ5 μm MPs (5MP) was administered alone or in combination with TBT to investigate the health risk of oral exposure in mice. All three treatments induced inflammation in the liver, altered gut microbiota composition and disturbed fecal bile acids profiles. In addition to decreasing triglyceride (TG) and increasing aspartate aminotransferase (AST) and macrophage-expressed gene 1 (Mpeg1), 5MP induced hepatic cholestasis by stimulating the expression of the cholesterol hydroxylase enzymes CYP8B1 and CYP27A1, and inhibiting multidrug resistance-associated protein 2 and 3 (MRP2, MRP3), and bile-salt export pump (BSEP) to prevent bile acids for entering the blood and bile. Correspondingly, 5MP treatment decreased 7-ketolithocholic acid (7-ketoLCA) and taurocholic acid (TCA), which were positively correlated with decreased *Bacteroides* and *Marvinbryantia* and negatively correlated with increased *Bifidobacterium*. In addition, TBT increased interferon γ (IFNγ) and Mpeg1 levels to induce inflammation, accompanied by decreased 7-ketoLCA, tauro-alpha-muricholic acid (T-alpha-MCA) and alpha-muricholic acid (alpha-MCA) levels, which were negatively related to *Coriobacteriaceae_UCG-002* and *Bifidobacterium*. Co-exposure to 5MP and TBT also decreased TG and induced bile acids accumulation in the liver due to inhibited BSEP, which might be attributed to the co-regulation of decreased T-alpha-MCA and *Harryflintia*. In conclusion, the administration of 5MP and TBT alone and in combination could cause gut microbiome dysbiosis and subsequently alter bile acids profiles, while the combined exposure of 5MP and TBT weakened the toxic effects of 5MP and TBT alone.

1. Introduction

Microplastics (MPs), a class of plastic particles or debris with diameters less than 5 mm (Wagner et al., 2014), are derived mainly from the degradation of plastic litter and globally exist in various environments, such as oceans (Peeken et al., 2018; van Wezel et al., 2016), air (Avio et al., 2017) and soil (Li et al., 2020; Wang et al., 2019). It has been proven that MPs are small enough to be mistakenly consumed by aquatic organisms and bioaccumulated in mammals through the food chain (Lusher et al., 2013). Additionally, MPs have been found in human feces (Schwabl et al., 2019). Numerous studies have revealed that MPs exposure cause toxicity to the physiological functions of marine organisms, including reduced feeding activity in *Arenicola marina* (Besseling et al., 2013), increased liver toxicity in zebrafish (Lu et al., 2016), enhanced neurotoxicity in *Pomatoschistus microps* (Luis et al., 2015), delayed growth in *Gammarus pulex* (Redondo-Hasselerharm et al., 2018) and decreased reproductive toxicity in oysters (Sussarellu et al., 2016). In addition to their toxicity, co-exposure of organisms in the environment to MPs with other chemical contaminants is a hot topic worthy of attention (Bradney et al., 2019; Fred-Ahmadu et al., 2020; Tourinho et al., 2019; Ziccardi et al., 2016). Most current studies have shown that MPs can adhere to other chemical contaminants and enhance their

* Correspondence to: Center for Global Health, School of Public Health, Nanjing Medical University, 101 Longmian Avenue, Nanjing 211166, PR China.
E-mail address: lilei@njmu.edu.cn (L. Li).
[1] These authors contributed equally to this work.

https://doi.org/10.1016/j.ecoenv.2021.112345
Received 19 January 2021; Received in revised form 11 May 2021; Accepted 12 May 2021
Available online 18 May 2021

ecotoxicological effects, such as increasing the adverse effects of polychlorinated biphenyls(PCBs) and polycyclic aromatic hydrocarbons (PAHs) in mussels (Rainieri et al., 2018). Importantly, a string of studies have reported that organotin is a kind of man-made heavy metal tin that is widespread in the marine environment (Cao et al., 2009; de Castro et al., 2012; Meng et al., 2009). Accordingly, co-exposure to MPs and organotin is inevitable (Romeo et al., 2015). Nevertheless, information on the toxicological interactions between MPs and organotin on organisms in the environment is scarce.

As the most widely used organotin type, tributyltin (TBT) has been applied as an antifouling agent for hull coatings, thermal stabilizer for plastic products, and chemical catalyst for textile products such as carpets (Arp et al., 2014). Additionally, TBT was reported to accumulate in the water and sediments due to its usage in other applications (Nowak et al., 2019). Aquatic organisms may be exposed to TBT via direct contact and inhalation of contaminated food and water (Castro et al., 2018; Kim et al., 2017; Laranjeiro et al., 2018). Although TBT-based compounds have been banned for use on ships, their residues in water still cause sex distortion, reproductive damage and survival impairment of aquatic organisms, even at quite low concentrations (Jordão et al., 2015; Khondee et al., 2016; Lee et al., 2019; Merlo et al., 2018). Furthermore, an investigation found that the TBT level in seafood collected from a market was 2.53 ng/g fresh weight (Rantakokko et al., 2006). According to statistics, fishermen's daily intake of seafood is between 94.1 and 250 g (Chien et al., 2002). Based on equivalent dose conversion, a 70 kg adult consuming 200 g seafood contaminated with TBT daily is approximately equal to the concentration of 100 ng/kg (body weight)/day TBT in mice. Thus, dietary intake of contaminated aquatic organisms and water is most likely the main route of simultaneous exposure to MPs and TBT for the general population (Smith et al., 2018). However, information on the effect of MPs and TBT co-exposure on mammals is limited.

Previous studies have demonstrated that both MPs and TBT could induce gut microbiota dysbiosis (Fackelmann and Sommer, 2019; Guo et al., 2018). The gut microbiota-bile acids crosstalk has also been proven to be associated with many physiological processes, such as inflammation (Adamovsky et al., 2018; Jia et al., 2018). In addition, bile acids (BAs) are synthesized from cholesterol in hepatocytes and are capable of regulating glucose and lipid metabolism through enterohepatic circulation (Alemán et al., 2018). In mammals, BAs are divided into primary and secondary BAs (Chen et al., 2019); primary BAs are mainly synthesized in the liver through cholesterol metabolism, and secondary BAs are produced from primary BAs through bacterial metabolism in the intestinal tract (Kiriyama and Nochi, 2019; Molinero et al., 2019). Nevertheless, the effect and underlying mechanisms of co-exposure of MPs and TBT on intestinal flora and BAs have not been reported. Polystyrene is one of most produced and commonly reported types of MPs in the environment (de Sa et al., 2018). A preliminary study certified that polystyrene MPs with a 5 μm diameter (Φ5 μm MPs) at a concentration of 0.1 mg/day could reach different tissues (liver and gut) with a steady state in mice (Jin et al., 2019). In the present study, we chose 5MP of polystyrene (0.1 mg/day) and TBT (100 ng/kg (body weight)/day) alone or in combination and studied their effects on intestinal microbiota composition and BAs profiles in C57BL/6J mice by integrating 16S rRNA sequencing of the gut microbiome and the metabolomics of BAs.

2. Material and methods

2.1. Chemicals

Polystyrene microplastics (MPs) particles were purchased from the BaseLine ChromTech Research Centre (Tianjin, China). Tributyltin chloride (TBT) was purchased from Dr. Ehrenstorfer, Laboratory of the Government Chemist (Teddington, UK), with 98% purity. Φ5 μm MPs was simplified to 5MP in our study. The dilution medium for 5MP and TBT was 0.4% ethyl alcohol in deionized water.

2.2. Animal models

Seven-week-old male C57BL/6J mice were obtained from Shanghai Sippr-BK Laboratory Animal Co., Ltd., and passed the ethical review of IACUC (No. 1812027). All mice were randomly divided into four groups, with ten mice in each group, which received different treatments by gavage. The four groups were exposed to control (100 μL of 0.4% ethyl alcohol), TBT (100 ng/kg (body weight)/day TBT), 5MP (0.1 mg/day 5MP), or 5MP+TBT (0.1 mg/day 5MP+100 ng/kg (body weight)/day TBT), respectively. During cultivation, there were no restrictions on food and water, and the light/dark (L/D) photoperiod was 12/12 h. During the exposure, the body weight of each mouse was recorded every 3 days from the first day of administration. Fecal samples were collected for 16S rRNA sequencing of the gut microbiome on the 33rd day. All mice were sacrificed after 12 h of starvation on the last day of the experiment. The collected blood was placed at room temperature for 2 h and centrifuged at 4000 rpm for 15 min to collect the serum, which was stored at − 80 °C. The liver was excised immediately and then divided: some sections of liver were fixed and sliced for further histological analysis, and the rest was stored at − 80 °C until use.

2.3. Biochemical parameters analysis of serum

Serum biochemical indexes, including triglyceride (TG) and aspartate aminotransferase (AST), in serum (n = 10) were detected by an automatic biochemical analyzer (Hitachi 7100, Tokyo, Japan).

2.4. Histopathology

Tissues (n = 3) were fixed with 4% paraformaldehyde for 24 h, embedded in paraffin, cut into at least two 5 μm thick sections and mounted on slides. The pathological changes in tissues were examined by hematoxylin and eosin (H&E) staining. Using Pannoramic SCAN (3DHISTECH, Budapest, Hungary), the stained slides were scanned by a blind method according to the standard method to obtain representative images.

2.5. RNA extraction and real-time quantitative PCR (RT-qPCR)

Total RNA was extracted using the FastPure Cell/Tissue Total RNA Isolation Kit (Vazyme, Biotech) and reverse transcribed into cDNA using HiScript II Q RT SuperMix (Vazyme, Biotech) following the manufacturer's instructions. The concentration and purity of total RNA and cDNA were detected using a NanoDrop2000 spectrophotometer (Thermo Fisher Scientific, MA, USA). Then, real-time PCR with a 10 μL mixture of Hieff quantitative PCR SYBR Green Master Mix (5 μL, Yeasen, Shanghai, China), forward primer, reverse primer (0.2 μM, see Supplement Material Table S1 for oligonucleotide sequences) and enriched cDNA was used to quantitatively detect the expression of genes (n = 6). The mixture was subjected to qPCR on a Light Cycler 480 (Roche, Shanghai). RT-qPCR analysis was performed in triplicate, and the $2^{-\Delta\Delta Ct}$ method was used to assess the relative expression level.

2.6. Measurement of TBA in serum, liver and feces

The levels of total bile acids (TBA) in serum, liver (n = 10) and feces (n = 6) were detected using a mouse TBA ELISA kit (Ren Jie Bio, Shanghai, China) according to the manufacturer's protocol.

2.7. Targeted determination of BAs using LC/MS

2.7.1. Extraction of metabolites in fecal samples

Precisely 10 mg of fecal sample from each group (n = 6) was placed in a 2 mL Eppendorf tube; 1 mL of methanol was added, and the solution

was vortexed for 1 min. Then, 100 mg of glass beads were added and shaken at 25 Hz for 60 s, and the above operation was repeated at least 2 times. The mixture was sonicated at room temperature for 30 min and centrifuged at 4 °C for 10 min (12,000*g*); 100 μL of the supernatant was added to 400 μL of methanol and vortexed for 30 s. A total of 300 μL of the supernatant was filtered through a 0.22 μm membrane, and the filtrate was added to a test bottle.

2.7.2. Instrument conditions

The chromatographic conditions were as follows: column, ACQUITY UPLC® BEH C_{18} Column (2.1 × 100 mm, 1.7 μm, Waters, American); injection volume, 5 μL; column temperature, 40 °C; mobile phase A, 0.01% formic acid water; mobile phase B, acetonitrile. The gradient elution conditions were as follows: 0 ~ 4 min, 25% B; 4 ~ 9 min, 25~30% B; 9 ~ 14 min, 30~36% B; 14 ~ 18 min, 36~38% B; 18 ~ 24 min, 38~50% B; 24 ~ 32 min, 50~75% B; 32 ~ 35 min, 75~100% B; 35 ~ 38 min, 100~25% B. The flow rate was 0.25 mL/min.

2.7.3. Mass spectrometry conditions

The electrospray ionization (ESI) source was negative ion mode. The ion source temperature was 500 °C, the ion source voltage was − 4500 V, the collision gas was 6 psi, the air curtain gas was 30 psi, and the atomizing gas and auxiliary gas were both 50 psi. Scanning was performed using multiple reaction monitoring (MRM).

The detailed information and methodological data of BAs were attached in Supplement Material Table S2.

2.8. Microbial community analysis

Microbial DNA from fecal samples of mice (n = 6) was extracted for 16S rRNA sequencing on an Illumina MiSeq platform (Illumina, San Diego, USA) according to our previous studies (Zhang et al., 2016). Then, the data were analyzed following the standard protocol by Majorbio Bio-Pharm Technology Co., Ltd. (Shanghai, China). Raw fastq files were quality-filtered by Trimmomatic and merged by FLASH with the following criteria: (i) The reads were truncated at any site with an average quality score < 20 over a 50 bp sliding window. (ii) Sequences whose overlap was longer than 10 bp were merged according to their overlap with a mismatch of no more than 2 bp. (iii) Sequences of each sample were separated according to barcodes (exactly matching) and primers (allowing 2 nucleotide mismatches), and reads containing ambiguous bases were removed. Operational taxonomic units (OTUs) were clustered with 97% similarity cutoff using UPARSE (version 7.1 http://drive5.com/uparse/) with a novel 'greedy' algorithm that performs chimera filtering and OTU clustering simultaneously. The taxonomy of each 16S rRNA gene sequence was analyzed by the RDP Classifier algorithm (http://rdp.cme.msu.edu/) against the Silva (SSU123) 16S rRNA database using a confidence threshold of 70%.

2.9. Statistical analysis

Data and diagrams in this study are expressed as the mean ± standard error of the mean (SEM). Differences between groups were analyzed by one-way analysis of variance (ANOVA) based on the least significant difference (LSD) test. A *P* value lower than 0.05 was considered statistically significant. Special and specific analyses are presented in the legend of each corresponding chart.

3. Results

3.1. Effect of single and combined 5MP and TBT exposure on body weight and TG and AST in serum

All mice were alive after 33 days of single and combined 5MP and

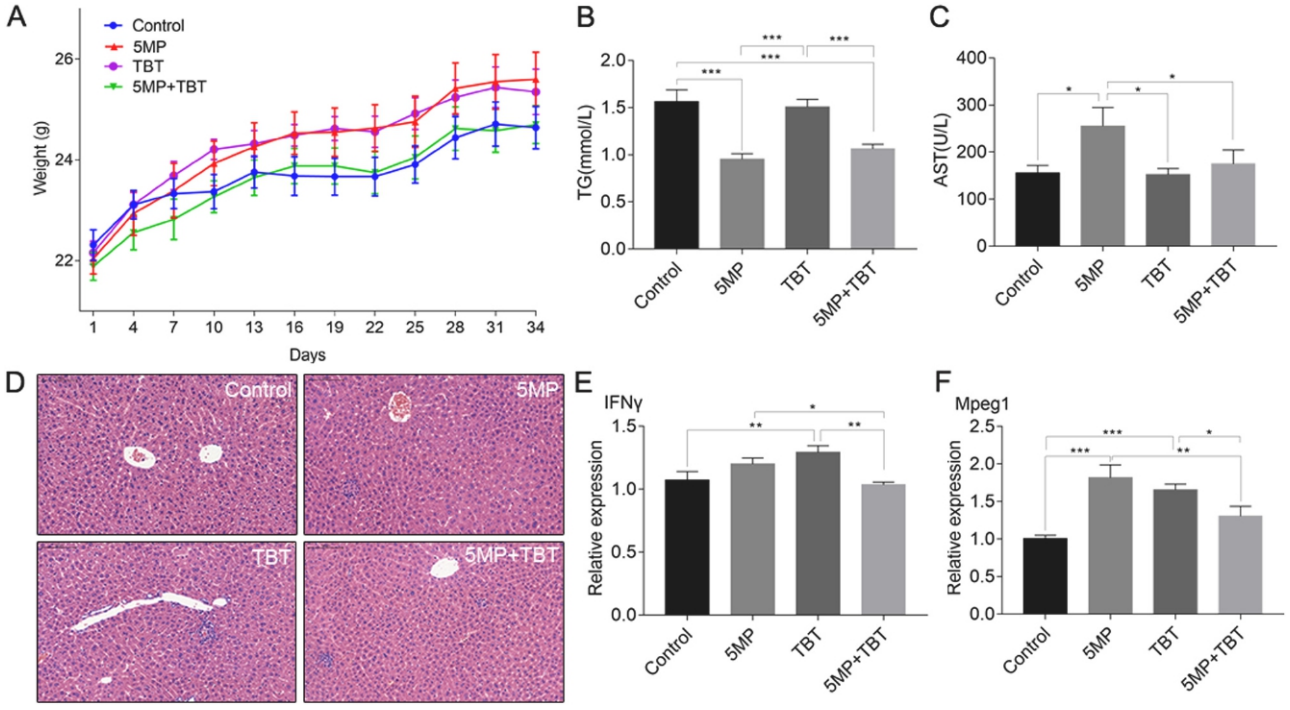

Fig. 1. Effect of administration of 5MP, TBT and their combination on (A) body weight, (B) the serum concentration of TG and (C) the serum level of AST. (D) Representative photomicrographs of liver tissue (scale bar, 100 μm; original magnification, 20×) after H&E staining. Inflammatory cell aggregation (shown by the black arrow) was observed in the liver. RT-qPCR results of RNA extracted from the liver showed the expression of the proinflammatory cytokine IFNγ (E) and the macrophage marker Mpeg1 (F) in each treatment group (*$P < 0.05$, **$P < 0.01$, ***$P < 0.001$).

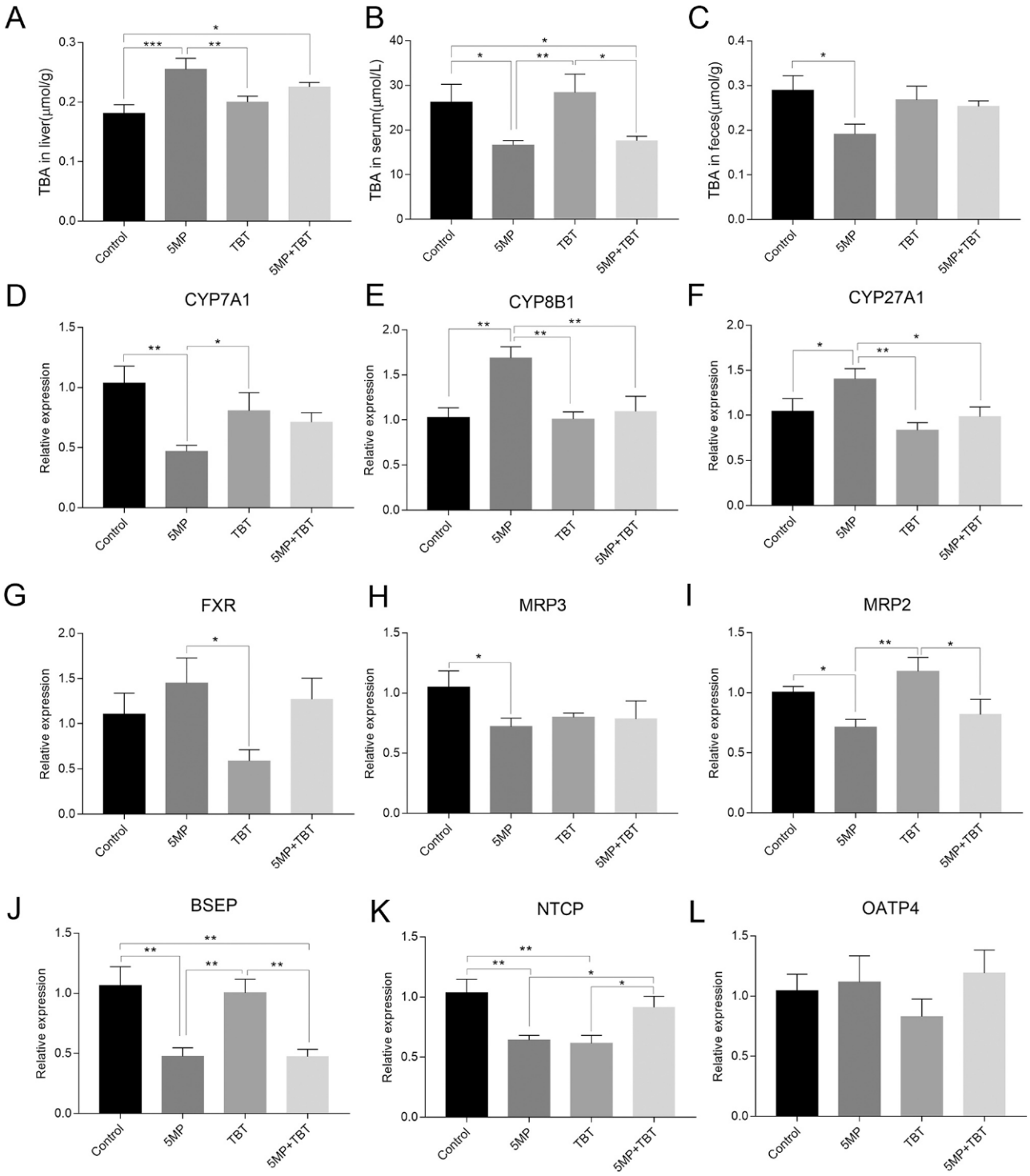

Fig. 2. Influence of 5MP and TBT alone or in combination on the total bile acids. The content of total bile acids (TBA) in the liver (A), serum (B) and feces (C). The expression of gene CYP7A1 (D), CYP8B1 (E), CYP27A1 (F), FXR (G), MRP3 (H), MRP2 (I), BSEP (J) and NTCP (K) OATP4 (L) in the liver (*$P < 0.05$, **$P < 0.01$, ***$P < 0.001$).

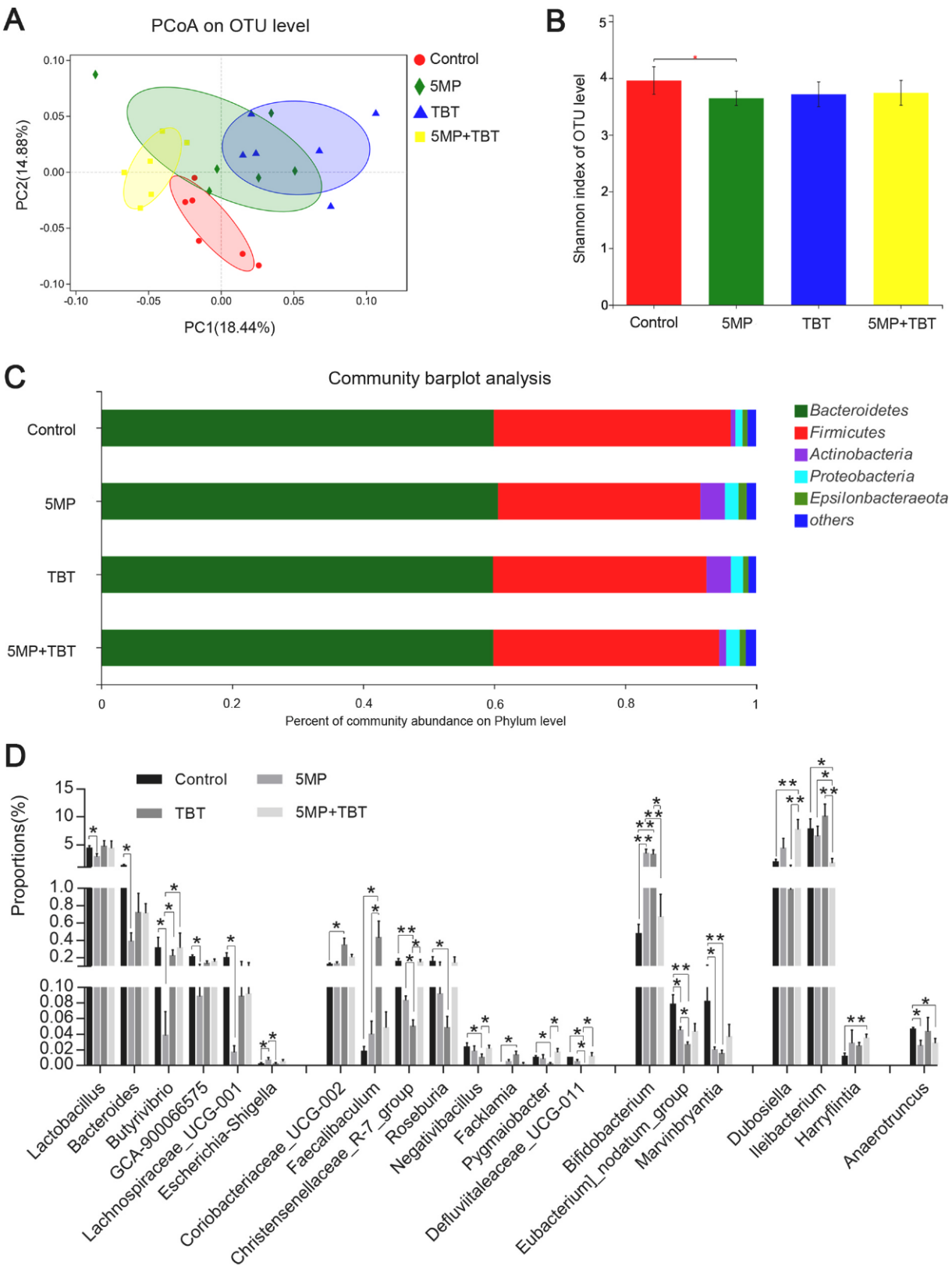

Fig. 3. 5MP and TBT alone or in combination alter intestinal microbiome composition. (A) Principal coordinate analysis (PCoA) based on Binary-lennon analysis (beta diversity) on operational taxonomic units (OTUs) (n = 6). Each symbol representing a single sample was colored according to each treatment. (B) The alpha diversity analysis of the Shannon index of the four treatments at the OTU level using the Wilcoxon rank-sum test. (C) Barplot of community abundance in the four groups at the phylum level. (D) The proportion of the gut microbiome at the genus level. Differences in each group were analyzed by the Wilcoxon rank-sum test. $^{*}P < 0.05$, $^{**}P < 0.01$, $^{***}P < 0.001$. (For interpretation of the references to color in this figure legend, the reader is referred to the web version of this article.)

TBT exposure. No significant difference in final weight was observed among each treatment group (Fig. 1 A). Compared to the control, 5MP and 5MP+TBT exposure notably decreased the level of serum TG, whereas no change was detected after TBT exposure, as shown in Fig. 1 B. In addition, the level of serum AST increased in the 5MP group compared with the control group (Fig. 1 C). Nevertheless, no significant differences of AST level were detected in TBT and 5MP+TBT exposure compared to control group (Fig. 1 C).

3.2. Histological lesions of the liver and transcription of related inflammatory factors and inflammatory cell markers

Histological observation indicated that single and combined 5MP and TBT exposure induced inflammation in the liver with aggregation of inflammatory cells (Fig. 1 D). RT-qPCR detected the relative expression of the corresponding inflammatory cytokine IFNγ and macrophage-labeled Mpeg1. The results showed that IFNγ in the liver of the TBT group (1.29 ± 0.05) was significantly increased compared to that of the control group (1.07 ± 0.07) (Fig. 1 E). In addition, the expression of Mpeg1 was significantly increased after 5MP (1.82 ± 0.17) and TBT (1.66 ± 0.07) exposure compared with the control (1.01 ± 0.04), indicating that the two separate exposures stimulated the Mpeg1 response (Fig. 1 F). Notably, the expression of IFNγ and Mpeg1 in 5MP+TBT showed no difference relative to the control but was significantly decreased compared to the separate treatments (Fig. 1 E and F).

3.3. Effect of single or combined 5MP and TBT exposure on TBA

As shown in Fig. 2 A, 5MP and 5MP + TBT interventions statistically up-regulated the content of TBA in the liver, while TBT treatment showed a non-significant change in TBA compared with the control group. Likewise, there was no obvious change in TBA in serum under TBT treatment (Fig. 2 B). However, 5MP and 5MP+TBT exposure visibly decreased serum TBA levels compared with the control group (Fig. 2 B). Moreover, the TBA in feces notably decreased in the 5MP group, indicating that the excretion of BAs was reduced in the 5MP group (Fig. 2 C). Intriguingly, 5MP treatment inhibited the expression of CYP7A1 and activated the expression of CYP8B1 and CYP27A1, while TBT and 5MP+TBT did not cause significant changes in these three genes (Fig. 2 D–F). Meanwhile, the BA-activated nuclear receptor FXR in 5MP increased compared to the control group, although it was not significant (Fig. 2 G). In addition, 5MP reduced the expression of MRP3 and MRP2, and both 5MP and 5MP+TBT suppressed the expression of BSEP (Fig. 2 H–J). Both 5MP and TBT inhibited NTCP whereas OATP4 showed no obvious change (Fig. 2 K and L). So 5MP mainly caused the increase of TBA in liver by activating CYP8B1 and CYP27A1 and inhibiting MRP3, MRP2 and BSEP, and 5MP+TBT induced hepatic cholestasis by inhibiting BSEP. Thus, we speculated that 5MP and TBT alone and in combination could affect the changes of TBA in mice through genes that regulate the synthesis and transport of BAs in the liver.

3.4. 5MP alone or in combination with TBT reshape microbiome composition

The intestinal environment was influenced by enterohepatic circulation of BAs by controlling the growth and maintenance of commensal gut microbiota. To determine the change in the gut microbiome in the control and three treatment groups, we used 16S rRNA-based high-throughput sequencing technology to detect the fecal microbiota composition in mouse feces. By analyzing the differences in each group by principal coordinate analysis (PCoA) (Fig. 3A), we found that the microbial communities in the 5MP, TBT and 5MP+TBT groups were dispersed compared to that in the control (Adonis test: $R^2 = 0.2711$, $P = 0.001$), which suggested that the microbial composition of each treatment group was not similar. Consistently, the alpha diversity of the gut microbiome was significantly lower in the 5MP group than in the control group based on the Shannon index, which further proved that 5MP could reduce microbiota diversity (Fig. 3 B). Although the Shannon indexes of TBT and 5MP+TBT showed no difference compared to that of the control, the barplot of community abundance at the phylum level showed that single or co-treatment with 5MP and TBT altered the composition of the gut microbiota (Fig. 3 C). The abundance of *Actinobacteria* increased from 0.72% in the control group to 3.74% and 3.73% in 5MP and TBT, respectively, whereas it returned to 1.07% in the 5MP+TBT group. The relative abundance of *Firmicutes* was 36.17% in the control group, and it decreased to 30.90% and 32.62% in the 5MP and TBT groups, respectively, while with the combined treatment (5MP+TBT), the value decreased to 34.47%. Both *Proteobacteria* and *Epsilonbacteraeota* were increased in the three treatment groups. Furthermore, at the genus level, differential genera were selected to study the dynamic changes induced by 5MP, TBT and their combined exposure (Fig. 3 D). Compared to the control group, *Lactobacillus*, *Bacteroides*, *Butyrivibrio*, *GCA-900066575* and *Lachnospiracea_UCG-001* significantly decreased and *Escherichia-Shigella* noticeably increased under 5MP exposure, but no difference in these genera appeared in the TBT or 5MP+TBT groups. TBT treatment obviously increased *Coriobacteriaceae_UCG-002*, *Faecalibaculum* and *Facklamia* and decreased *Roseburia*, *Christensenellaceae_R-7_group*, *Negativibacillus*, *Pygmaiobacter*, and *Defluviitaleaceae_UCG-001* relative to the control; however, these genera were not affected in the 5MP and 5MP+TBT groups. Moreover, both 5MP and TBT significantly increased *Bifidobacterium* and markedly decreased *Eubacterium]_nodatum_group* and *Marvinbryantia*, but no obvious differences were found between the control and 5MP+TBT groups. *Dubosiella* and *Harryflintia* were increased and *Ileibacterium* was decreased significantly under 5MP+TBT exposure, but no remarkable changes were observed in the 5MP and TBT groups compared with the control group. In addition, *Anaerotruncus* was inhibited in both the 5MP and 5MP+TBT groups. These results illustrated that all of the above treatments could shape the community of the mouse gut microbiome in different ways.

3.5. Influence of 5MP alone or in combination with TBT on the fecal BAs profiles

Since feces is a type of easily accessible and noninvasive biological sample that could also reflect the detail BAs level, we performed targeted quantitative detection to identify specific BAs in feces that were specifically regulated by 5MP, TBT and their combined exposure. The composition of primary BAs and secondary BAs showed obvious changes in the three treatment groups relative to the control (Fig. 4 A). As presented in Fig. 4 B, compared with the control, 5MP obviously inhibited TCA and 7-ketoLCA, and TBT visibly decreased 7-ketoLCA, T-alpha-MCA, 12-ketoLCA, and alpha-MCA. Notably and intriguingly, the combination of 5MP and TBT significantly decreased T-alpha-MCA. In short, these results clearly showed that the composition of primary and secondary BAs fluctuated after 5MP exposure alone or in combination with TBT.

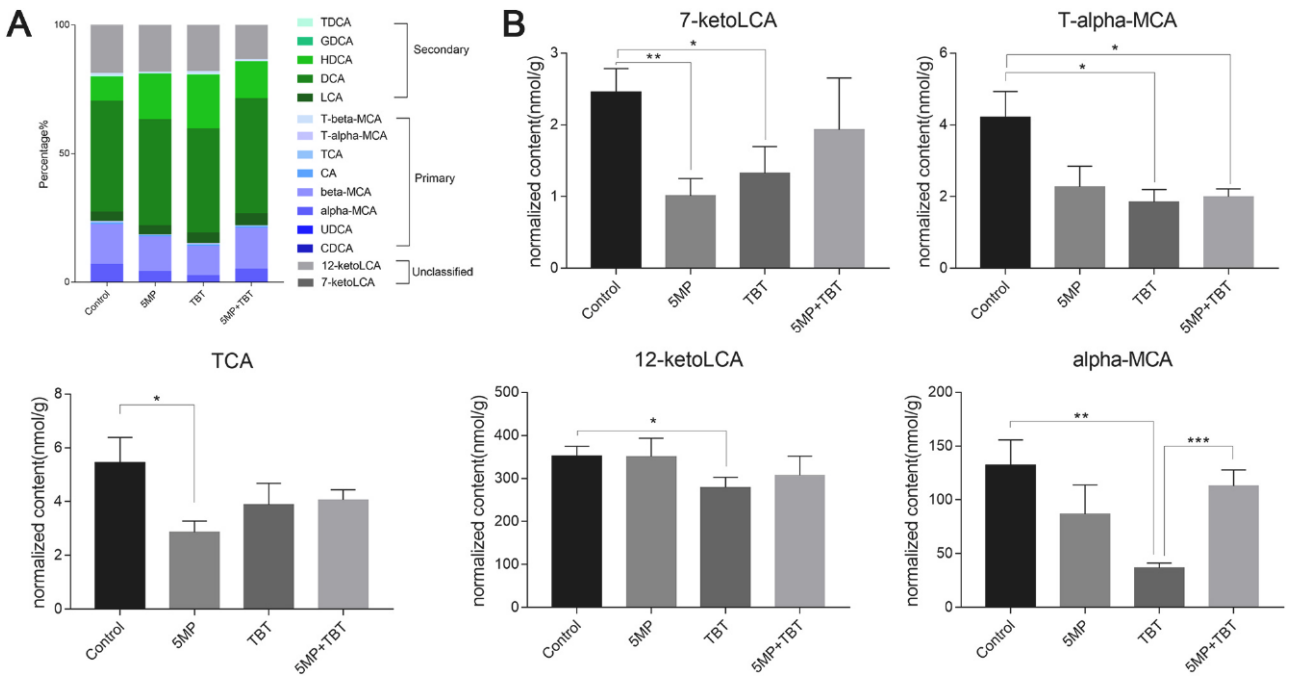

Fig. 4. Influence of 5MP and TBT alone or in combination on the fecal bile acids (BAs) profiles. (A) The composition of primary and secondary BAs. (B) Detailed BAs changes of 5MP and TBT alone or in combination. Two groups with fold change ≥ 1.5 and $P < 0.05$ (Student's *t*-test) were considered to be significantly different. $^{*}P < 0.05$, $^{**}P < 0.01$, $^{***}P < 0.001$.

3.6. Crosstalk between BAs and fecal bacteria under single or combined 5MP and TBT treatments

Given the possible relationships between the intestinal microbiome and altered BAs, we further explored crosstalk through correlation analysis, as shown in Fig. 5. The results showed that differences in BAs were significantly related to intestinal bacteria under different treatments. According to the results in Fig. 3 D and Fig. 4 B, decreased levels of *Bacteroides* and *Marvinbryantia* were positively correlated and increased *Bifidobacterium* was negatively correlated with decreased 7-ketoLCA and TCA in the 5MP group. *Lachnospiraceae_UCG-001* was positively related to decreased TCA in the 5MP group. In addition, increased levels of *Coriobacteriaceae_UCG-002* and *Bifidobacterium* showed a negative relation with decreased 7-ketoLCA and T-alpha-MCA in the TBT group. *Christensenellaceae_R-7_group* and *Marvinbryantia* were positively related to T-alpha-MCA, and *Coriobacteriaceae_UCG-002, Pygmaiobacter, Defluviitaleaceae_UCG-001* and *Eubacterium]_nodatum_group* were positively related to alpha-MCA in the TBT group. In addition, T-alpha-MCA was negatively related to *Harryflintia* in the 5MP+TBT group. In summary, the changes in BAs induced by single or combined administration of 5MP and TBT were inseparable from the regulation of intestinal bacteria.

4. Discussion

In this study, exposure to 5MP, TBT and 5MP+TBT did not significantly change the body weight of C57BL/6J mice, indicating that an adaptive response mechanism to 5MP (0.1 mg/day) and TBT (100 ng/kg (body weight)/day) existed (Fig. 1 A). The content of TBA in 5MP and 5MP + TBT groups statistically increased compared with control group, but that was opposite in serum (Fig. 2 A–C). These data suggested that 5MP and 5MP+TBT might induce BA accumulation in the liver. It was reported that BAs are synthesized in hepatocytes via cytochrome P450-mediated oxidation of cholesterol (Jia et al., 2018). Although the bile acid synthesize rate-limiting enzyme (CYP7A1) was reported as a key member enzyme for the classical pathway of BA synthesis, the absence of CYP7A1 did not affect the elimination of BAs (Beigneux et al., 2002). In our study, we found that CYP7A1 gene was inhibited in 5MP group (Fig. 2 D–F). Instead, 5MP treatment led to increased liver TBA (Fig. 2 A) by up-regulating the enzymatic gene CYP8B1 and the alternative pathway BA synthesis gene CYP27A1 as shown in Fig. 2 E and F. Moreover, BAs could be secreted into the portal circulation via basolateral BA transporters MRP3, into bile via canalicular export transporters BSEP and MRP2 (Jia et al., 2018; Kubitz et al., 2015). Inhibition of MRP3 in the 5MP group revealed a decreasion of BAs excreted into the blood from the liver (Fig. 2 B and H), and down-regulation of MRP2 and BSEP indicated a decrease in BAs entering the bile, which also be responsible for lower TBA in the feces (Fig. 2 C, I and J). All the data indicated that 5MP exposure led to hepatic cholestasis. Additionally, it has been reported that hepatic cholestasis leads to toxic BAs and that other metabolites accumulate in the liver, causing hepatitis and damage (Zollner and Trauner, 2008), which explains why 5MP-induced hepatic cholestasis could result in inflammation in the liver (Fig. 1 D). As shown in Fig. 1 F, 5MP increased the expression of Mpeg1, revealing that mice developed hepatic immunity due to exposure to 5MP. Meanwhile, *Escherichia-Shigella*, which is certified as a pro-inflammatory strain, could induce inflammation. A previous study identified that *Escherichia-Shigella* was positively correlated with the serum liver function marker AST (Lu et al., 2019). Our study consistently found that 5MP increased the proportion of *Escherichia- Shigella* accompanied by remarkably elevated AST level (Fig. 1 C and Fig. 3 D). Furthermore, *Bacteroides* was reported to be positively correlated with blood TG (Liu et al., 2020). Lipopolysaccharides, as one of the components of *Bacteroides,* could reduce the level of TG (Jiang et al., 2018; Liu et al., 2019a), further providing evidence that 5MP might inhibit *Bacteroides* to regulate the level of TG (Fig. 1 B and Fig. 3 D). *Lactobacillus* and *Bacteroides* were reported to be responsible for biotransformation between conjugated and deconjugated BAs via bile salt hydrolase (Wexler, 2007). In this study, we found that TCA was positively correlated with *Bacteroides* (Fig. 5). Moreover, oral supplementation with TCA could notably reduce TG (Janssen et al., 2017), which corresponds to our results that 5MP decreased TCA excretion in feces accompanied by a decrease in *Bacteroides* (Fig. 3 D and Fig. 4 B). Moreover, TCA was shown to be involved in the absorption of cholesterol by bile salt hydrolase-rich *Bifidobacterium,*

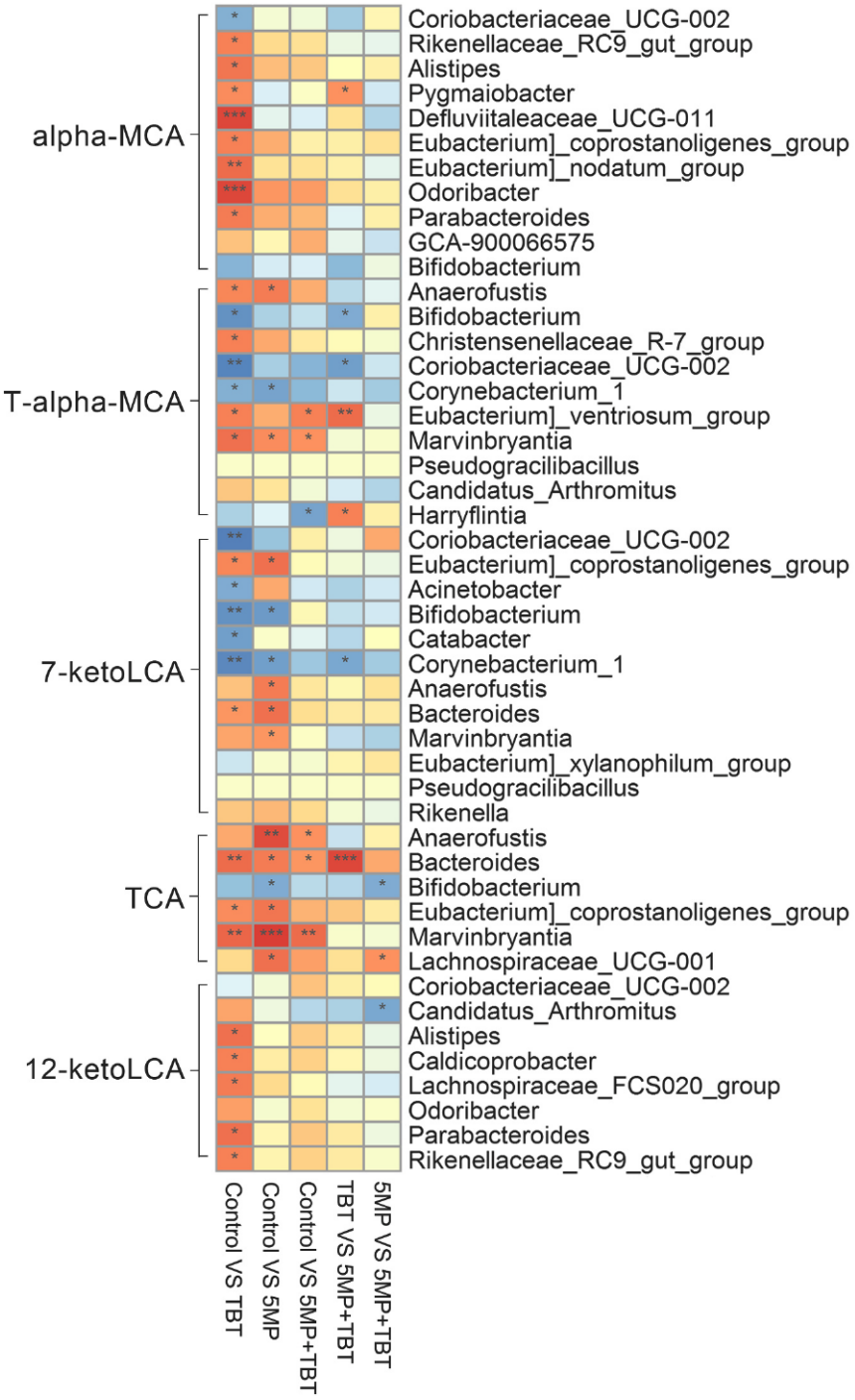

Fig. 5. Crosstalk of bile acids (BAs) and fecal bacteria under sole or combined 5MP and TBT treatments. Differential BAs were screened according to different treatments based on pairwise comparisons. Differential genera of the gut microbiome were screened according to different treatments based on the Wilcoxon rank-sum test. BAs and flora with *P* values less than 0.05 were considered significantly different. Pearson correlation analysis was performed on the BAs and flora that were found to be significantly different according to the treatment, and a heat map was formed; only significant correlations were presented in the map. Significant squares are marked with *, $*P < 0.05$, $**P < 0.01$, $***P < 0.001$.

the colonization of which could reduce blood and liver fat content in mice fed a high-fat diet (Hu et al., 2014; Tahri et al., 1997), suggesting that the increase in *Bifidobacterium* might lead to down-regulation of TCA in the 5MP group. These data indicated that 5MP could induce a decrease in TCA and TG levels by crosstalk with a decrease in *Bacteroides* and an increase in *Bifidobacterium*.

Consistent with previous reports (Bertuloso et al., 2015; Mitra et al., 2014), TBT treatment caused liver inflammation (Fig. 1 D), and further cytokine detection demonstrated that TBT induced an increase in IFNγ and Mpeg1 to activate immune prevention. TBT was found to increase the proportion of *Facklamia, Coriobacteriaceae_UCG-002*, and *Faecalibaculum* and decrease *Roseburia* and *Christensenellaceae_R-7_group* (Fig. 3 D). These altered genera were reported to be involved in host health. For instance, *Facklamia*, as an underrecognized pathogen, could cause infection in susceptible hosts and induce endocarditis (Rahmati et al., 2017). *Faecalibaculum* is a well-described anti-inflammatory organism associated with inflammation in patients with Crohn disease (Sokol et al., 2008). Additionally, *Coriobacteriaceae* was reported to be abundant in children and adolescents with obesity, which is considered low-grade chronic inflammation and positively correlated with fecal reactive oxygen species (ROS) to induce inflammation (Qasem et al., 2017). A previous study verified that a high-fat diet caused colonic and hepatic inflammation in mice with inhibited *Christensenellaceae_R-7_group* (Liu et al., 2019b). Moreover, the butyrate-producing genus *Roseburia* can be used as a probiotic to alleviate endotoxemia and improve immunological disorders and gut barrier function

(Patterson et al., 2017). Consequently, changes in the proportion of those genera might play important roles in TBT-induced hepatic inflammation. Meanwhile, we did not observe a change in TBA in the TBT group, but we found that TBT inhibited 12-ketoLCA, 7-ketoLCA, T-alpha-MCA and alpha-MCA in feces (Fig. 4 D), and the reduction in 7-ketoLCA and T-alpha-MCA showed a negative relation with *Coriobacteriaceae_UCG-002* and *Bifidobacterium* (Fig. 5). A previous study determined that *Coriobacteriaceae_UCG-002* could affect steroid and bile salt metabolism and reduce cholesterol fecal excretion by increasing BA absorption (Romo-Vaquero et al., 2019). The bile salt hydrolyzing enzymes of *Coriobacteriaceae_UCG-002* may initiate an important detoxification mechanism and prevent the antibacterial properties of some BAs (Clavel et al., 2014; Doden et al., 2018). These data suggested that 7-ketoLCA, T-alpha-MCA and alpha-MCA might coregulate *Coriobacteriaceae_UCG-002* and *Bifidobacterium* to respond to the stimulus of TBT.

Although we did not observe a significant increase in BAs-related gene CYP8B1 and CYP27A1 expression, hepatic cholestasis was induced by co-exposure to 5MP and TBT (Fig. 2 A, E and F). Except that the inhibition of BSEP prevented the excretion of BAs into bile, the uptake transporter NTCP was not affected, which is also a reasonable explanation for cholestasis in 5MP+TBT (Fig. 2 A, I and J). 5MP+TBT did not promote the synthesis of BAs, and prevented the efflux of BAs by inhibiting BSEP, causing intrahepatic stasis, so the content of intrahepatic bile was lower than that of the 5MP group. In addition, we also found that 5MP+TBT did not cause a significant increase in AST, IFNγ or Mpeg1 as 5MP and TBT alone did. Interestingly, significant differences in gut microbiota and bile acids were altered under exposure to 5MP and TBT alone and in combination. The results showed that 5MP altered 7-ketoLCA and TCA (Fig. 4 B), and *Lactobacillus, Bacteroides, Escherichia-Shigella,* and *Bifidobacterium* etc (Fig. 3 D). In addition, TBT changed 7-ketoLCA, 12-ketoLCA, and alpha-MCA (Fig. 4 B), and *Coriobacteriaceae_UCG-002, Pygmaiobacter, Bifidobacterium* etc (Fig. 3 D); however, the above changes did not occur in the 5MP+TBT group. According to previous studies, MPs can adsorb metals, metalloids, antibiotics and persistent organic pollutants in polluted aquatic environments (Imran et al., 2019). However, the potential bioavailability of metals associated with plastic particles will depend on their physical and chemical form within the particle body, particle size, and exposure time. According to our measurement of total tin in the liver (Supplement Material Fig. S1), it was indeed found that the total tin level of 5MP+TBT was nearly 30% lower than that of the TBT group, which might be a plausible explanation for the above phenomenon in different treatments. While in this study, co-exposure to 5MP and TBT increased *Dubosiella* and *Harryflintia* and decreased *Ileibacterium* and *Anaerotruncus* in the gut microbiota. *Anaerotruncus* is a butyrate producer that was effective in the treatment of inflammatory bowel diseases (Wang et al., 2018), and it was inhibited under 5MP+TBT exposure in this study. Our findings indicated that decreased T-alpha-MCA was positively related to *Harryflintia* in the TBT+5MP group. T-alpha-MCA is an FXR antagonist that can be decomposed by bacterial cholate hydrolase to form alpha-MCA and BAs that are not reabsorbed by ASBT excreted with feces (de Aguiar Vallim et al., 2013). *Harryflintia*, a genus of the family *Ruminococcaceae*, grows on chitin as the only carbon resource (Li et al., 2017). Additionally, the water-insoluble dietary fiber chitin decreased bile acid excretion in rats (Ide et al., 1990). Therefore, we speculated that the combination of 5MP and TBT might increase *Harryflintia* and inhibit T-alpha-MCA excretion.

In conclusion, the influence and mechanisms in response to 5MP, TBT and their combined exposure were regulated by crosstalk of the intestinal microbiota and BAs profiles. 5MP stimulated the expression of CYP8B1 and CYP27A1 to induce hepatic cholestasis and prevented BAs for entering the blood and bile by inhibiting MRP3, MRP2 and BSEP. Decreased 7-ketoLCA and TCA in feces were positively related to *Bacteroides* and *Marvinbryantia* and negatively related to *Bifidobacterium*, which might be a factor of inflammation, decreased TG and elevated AST in the liver. In addition, TBT induced inflammation and increased IFNγ and Mpeg1, accompanied by inhibition of 7-ketoLCA, T-alpha-MCA and alpha-MCA, which were negatively related to *Coriobacteriaceae_UCG-002* and *Bifidobacterium*. The co-exposure of 5MP and TBT inhibited BSEP, which in turn induced BAs accumulation in the liver, and inhibited T-alpha-MCA excretion, which might be mediated by elevated *Harryflintia*. Our research revealed that 5MP and TBT alone and in combination could induce changes in the crosstalk between the gut microbiome and bile acid profile. However, the combined exposure of 5MP and TBT weakened the toxic effects of 5MP and TBT alone.

CRediT authorship contribution statement

Ping Jiang, Lei Li: Conceptualization. **Ping Jiang, Ge-hui Yuan, Bao-rong Jiang, Jing-yi Zhang , Yu-qian Wang, Hui-jie Lv, Zhan Zhang, Jia-lin Wu, Lei Li**: Data curation. **Ping Jiang, Ge-hui Yuan, Lei Li**: Formal analysis. **Ping Jiang**: Investigation. **Ping Jiang, Lei Li**: Funding acquisition. **Ping Jiang, Qian Wu, Lei Li**: Methodology. **Ping Jiang, Lei Li**: Resources. **Ping Jiang, Ge-hui Yuan**: Software. **Ping Jiang, Lei Li**: Supervision. **Lei Li**: Project administration. **Ping Jiang, Lei Li**: Validation. **Ping Jiang**: Visualization. **Ping Jiang, Ge-hui Yuan**: Writing - original draft. **Ping Jiang, Ge-hui Yuan, Lei Li**: Writing - review & editing.

Declaration of Competing Interest

The authors declare that they have no known competing financial interests or personal relationships that could have appeared to influence the work reported in this paper.

Acknowledgments

This work was supported by the National Natural Science Foundation of China (81673228, 81973096 and 82003504), The Natural Science Foundation of the Jiangsu Higher Education Institutions of China (19KJB330004), Science and Technology Development Fund of Nanjing Medical University (NMUB2019012).

Appendix A. Abbreviations.

MPs	microplastics
TBT	tributyltin
5MP	Φ5 μm microplastics
BAs	bile acids
TG	triglyceride
AST	aspartate aminotransferase
H&E	hematoxylin and eosin
RT-qPCR	real-time quantitative PCR
IFNγ	interferon-gamma
Mpeg1	macrophage expressed gene 1
CYP7A1	cholesterol 7α-hydroxylase

(*continued on next page*)

(*continued*)

CYP8B1	sterol 12α-hydroxylase gene
CYP27A1	sterol 27-hydroxylase
FXR	farnesoid X receptor
MRP3	multidrug resistance-associated protein 3
BSEP	bile salt export pump
MRP2	multidrug resistance-associated protein 2
NTCP	sodium taurocholate cotransporting polypeptide
OATP4	organic anion transporting polypeptide 4
ESI	electrospray ionization
MRM	multiple reaction monitoring
SEM	standard error of mean
ANOVA	analysis of variance
PCoA	principal co-ordinates analysis
LCA	lithocholic acid
12-ketoLCA	12-ketolithocholic acid
7-ketoLCA	7-ketolithocholic acid
DCA	deoxycholic acid
CDCA	chenodeoxycholic acid
UDCA	ursodeoxycholic acid
HDCA	hyodeoxycholic acid
alpha-MCA	alpha-muricholic acid
beta-MCA	beta-muricholic acid
CA	cholic acid
GDCA	glycodeoxycholic acid
THDCA	taurohyodeoxycholic acid
TUDCA	tauroursodeoxycholic acid
TDCA	taurodeoxycholic acid
TCA	taurocholic acid
T-alpha-MCA	tauro-alpha-muricholic acid
T-beta-MCA	tauro-beta-muricholic acid

Appendix B. Supporting information

Supplementary data associated with this article can be found in the online version at doi:10.1016/j.ecoenv.2021.112345.

References

Adamovsky, O., Buerger, A.N., Wormington, A.M., Ector, N., Griffitt, R.J., Bisesi JH, Jr, Martyniuk, C.J., 2018. The gut microbiome and aquatic toxicology: an emerging concept for environmental health. Environ. Toxicol. Chem. 37, 2758–2775.

de Aguiar Vallim, T.Q., Tarling, E.J., Edwards, P.A., 2013. Pleiotropic roles of bile acids in metabolism. Cell Metab. 17, 657–669.

Alemán, J.O., Bokulich, N.A., Swann, J.R., Walker, J.M., De Rosa, J.C., Battaglia, T., Costabile, A., Pechlivanis, A., Liang, Y., Breslow, J.L., Blaser, M.J., Holt, P.R., 2018. Fecal microbiota and bile acid interactions with systemic and adipose tissue metabolism in diet-induced weight loss of obese postmenopausal women. J. Transl. Med. 16, 244.

Arp, H.P., Eek, E., Nybakk, A.W., Glette, T., Møskeland, T., Pettersen, A., 2014. When will the TBT go away? Integrating monitoring and modelling to address TBT's delayed disappearance in the Drammensfjord, Norway. Water Res. 65, 213–223.

Avio, C.G., Gorbi, S., Regoli, F., 2017. Plastics and microplastics in the oceans: from emerging pollutants to emerged threat. Mar. Environ. Res. 128, 2–11.

Beigneux, A., Hofmann, A.F., Young, S.G., 2002. Human CYP7A1 deficiency: progress and enigmas. J. Clin. Investig. 110, 29–31.

Bertuloso, B.D., Podratz, P.L., Merlo, E., de Araújo, J.F., Lima, L.C., de Miguel, E.C., de Souza, L.N., Gava, A.L., de Oliveira, M., Miranda-Alves, L., Carneiro, M.T., Nogueira, C.R., Graceli, J.B., 2015. Tributyltin chloride leads to adiposity and impairs metabolic functions in the rat liver and pancreas. Toxicol. Lett. 235, 45–59.

Besseling, E., Wegner, A., Foekema, E.M., van den Heuvel-Greve, M.J., Koelmans, A.A., 2013. Effects of microplastic on fitness and PCB bioaccumulation by the lugworm Arenicola marina (L.). Environ. Sci. Technol. 47, 593–600.

Bradney, L., Wijesekara, H., Palansooriya, K.N., Obadamudalige, N., Bolan, N.S., Ok, Y. S., Rinklebe, J., Kim, K.H., Kirkham, M.B., 2019. Particulate plastics as a vector for toxic trace-element uptake by aquatic and terrestrial organisms and human health risk. Environ. Int. 131, 104937.

Cao, D., Jiang, G., Zhou, Q., Yang, R., 2009. Organotin pollution in China: an overview of the current state and potential health risk. J. Environ. Manag. 90 (Suppl 1), S16–24.

de Castro, I.B., Perina, F.C., Fillmann, G., 2012. Organotin contamination in South American coastal areas. Environ. Monit. Assess. 184, 1781–1799.

Castro, Í.B., Iannacone, J., Santos, S., Fillmann, G., 2018. TBT is still a matter of concern in Peru. Chemosphere 205, 253–259.

Chen, M.L., Takeda, K., Sundrud, M.S., 2019. Emerging roles of bile acids in mucosal immunity and inflammation. Mucosal Immunol. 12, 851–861.

Chien, L.C., Hung, T.C., Choang, K.Y., Yeh, C.Y., Meng, P.J., Shieh, M.J., Han, B.C., 2002. Daily intake of TBT, Cu, Zn, Cd and As for fishermen in Taiwan. Sci. Total Environ. 285, 177–185.

Clavel, T., Desmarchelier, C., Haller, D., Gérard, P., Rohn, S., Lepage, P., Daniel, H., 2014. Intestinal microbiota in metabolic diseases: from bacterial community structure and functions to species of pathophysiological relevance. Gut Microbes 5, 544–551.

Doden, H., Sallam, L.A., Devendran, S., Ly, L., Doden, G., Daniel, S.L., Alves, J., Ridlon, J. M., 2018. Metabolism of oxo-bile acids and characterization of recombinant 12α-hydroxysteroid dehydrogenases from bile acid 7α-dehydroxylating human gut bacteria. Appl. Environ. Microbiol. 84, 84.

Fackelmann, G., Sommer, S., 2019. Microplastics and the gut microbiome: how chronically exposed species may suffer from gut dysbiosis. Mar. Pollut. Bull. 143, 193–203.

Fred-Ahmadu, O.H., Bhagwat, G., Oluyoye, I., Benson, N.U., Ayejuyo, O.O., Palanisami, T., 2020. Interaction of chemical contaminants with microplastics: principles and perspectives. Sci. Total Environ. 706, 135978.

Guo, H., Yan, H., Cheng, D., Wei, X., Kou, R., Si, J., 2018. Tributyltin exposure induces gut microbiome dysbiosis with increased body weight gain and dyslipidemia in mice. Environ. Toxicol. Pharmacol. 60, 202–208.

Hu, X., Bonde, Y., Eggertsen, G., Rudling, M., 2014. Muricholic bile acids are potent regulators of bile acid synthesis via a positive feedback mechanism. J. Intern. Med. 275, 27–38.

Ide, T., Horii, M., Yamamoto, T., Kawashima, K., 1990. Contrasting effects of water-soluble and water-insoluble dietary fibers on bile acid conjugation and taurine metabolism in the rat. Lipids 25, 335–340.

Imran, M., Das, K.R., Naik, M.M., 2019. Co-selection of multi-antibiotic resistance in bacterial pathogens in metal and microplastic contaminated environments: an emerging health threat. Chemosphere 215, 846–857.

Janssen, A., Dijk, W., Boekhorst, J., Kuipers, F., Groen, A.K., Lukovac, S., Hooiveld, G., Kersten, S., 2017. ANGPTL4 promotes bile acid absorption during taurocholic acid supplementation via a mechanism dependent on the gut microbiota. Biochim. Biophys. Acta Mol. Cell Biol. Lipids 1862, 1056–1067.

Jia, W., Xie, G., Jia, W., 2018. Bile acid-microbiota crosstalk in gastrointestinal inflammation and carcinogenesis. Nat. Rev. Gastroenterol. Hepatol. 15, 111–128.

Jiang, Z., Zhao, M., Zhang, H., Li, Y., Liu, M., Feng, F., 2018. Antimicrobial emulsifier-glycerol monolaurate induces metabolic syndrome, gut microbiota dysbiosis, and systemic low-grade inflammation in low-fat diet fed mice. Mol. Nutr. Food Res. 62, 62.

Jin, Y., Lu, L., Tu, W., Luo, T., Fu, Z., 2019. Impacts of polystyrene microplastic on the gut barrier, microbiota and metabolism of mice. Sci. Total Environ. 649, 308–317.

Jordão, R., Casas, J., Fabrias, G., Campos, B., Piña, B., Lemos, M.F., Soares, A.M., Tauler, R., Barata, C., 2015. Obesogens beyond vertebrates: lipid perturbation by tributyltin in the crustacean Daphnia magna. Environ. Health Perspect. 123, 813–819.

Khondee, P., Srisomsap, C., Chokchaichamnankit, D., Svasti, J., Simpson, R.J., Kingtong, S., 2016. Histopathological effect and stress response of mantle proteome following TBT exposure in the Hooded oyster Saccostrea cucullata. Environ. Pollut. 218, 855–862.
Kim, T., Jeon, S., Hong, S., Song, S.J., Kwon, B.O., Ryu, J., Khim, J.S., 2017. Spatiotemporal distributions of butyltin compounds in various intertidal organisms along the Samcheok and Tongyeong coasts of Korea. Chemosphere 172, 268–277.
Kiriyama, Y., Nochi, H., 2019. The biosynthesis, signaling, and neurological functions of bile acids. Biomolecules 9, 9.
Kubitz, R., Dröge, C., Kluge, S., Stross, C., Walter, N., Keitel, V., Häussinger, D., Stindt, J., 2015. Autoimmune BSEP disease: disease recurrence after liver transplantation for progressive familial intrahepatic cholestasis. Clin. Rev. Allergy Immunol. 48, 273–284.
Laranjeiro, F., Sánchez-Marín, P., Oliveira, I.B., Galante-Oliveira, S., Barroso, C., 2018. Fifteen years of imposex and tributyltin pollution monitoring along the Portuguese coast. Environ. Pollut. 232, 411–421.
Lee, M.C., Fonseca, E., Park, J.C., Yoon, D.S., Choi, H., Kim, M., Han, J., Cho, H.S., Shin, K.H., Santos, M.L., Jung, J.H., Castro, L., Lee, J.S., 2019. Tributyltin affects retinoid X receptor-mediated lipid metabolism in the marine rotifer Brachionus koreanus. Environ. Sci. Technol. 53, 7830–7839.
Li, L., Luo, Y., Li, R., Zhou, Q., Peijnenburg, W.J.G.M., Yin, N., Yang, J., Tu, C., Zhang, Y., 2020. Effective uptake of submicrometre plastics by crop plants via a crack-entry mode. Nat. Sustain. 3, 929–937.
Li, Y., Zhang, L.L., Liu, L., Tian, Y.Q., Liu, X.F., Li, W.J., Dai, Y.M., 2017. Paludicola psychrotolerans gen. nov., sp. nov., a novel psychrotolerant chitinolytic anaerobe of the family Ruminococcaceae. Int. J. Syst. Evol. Microbiol. 67, 4100–4103.
Liu, B., Zhang, J., Sun, P., Yi, R., Han, X., Zhao, X., 2019a. Raw Bowl Tea (Tuocha) polyphenol prevention of nonalcoholic fatty liver disease by regulating intestinal function in mice. Biomolecules 9, 435.
Liu, W., Zhou, Y., Qin, Y., Li, Y., Yu, L., Li, R., Chen, Y., Xu, Y., 2020. Sex-specific effects of PM2.5 maternal exposure on offspring's serum lipoproteins and gut microbiota. Sci. Total Environ. 739, 139982.
Liu, Y., Li, T., Alim, A., Ren, D., Zhao, Y., Yang, X., 2019b. Regulatory effects of stachyose on colonic and hepatic inflammation, gut microbiota dysbiosis, and peripheral CD4(+) T cell distribution abnormality in high-fat diet-fed mice. J. Agric. Food Chem. 67, 11665–11674.
Lu, H.F., Ren, Z.G., Li, A., Zhang, H., Xu, S.Y., Jiang, J.W., Zhou, L., Ling, Q., Wang, B.H., Cui, G.Y., Chen, X.H., Zheng, S.S., Li, L.J., 2019. Fecal microbiome data distinguish liver recipients with normal and abnormal liver function from healthy controls. Front. Microbiol. 10, 1518.
Lu, Y., Zhang, Y., Deng, Y., Jiang, W., Zhao, Y., Geng, J., Ding, L., Ren, H., 2016. Uptake and accumulation of polystyrene microplastics in Zebrafish (Danio rerio) and toxic effects in liver. Environ. Sci. Technol. 50, 4054–4060.
Luís, L.G., Ferreira, P., Fonte, E., Oliveira, M., Guilhermino, L., 2015. Does the presence of microplastics influence the acute toxicity of chromium(VI) to early juveniles of the common goby (Pomatoschistus microps)? A study with juveniles from two wild estuarine populations. Aquat. Toxicol. 164, 163–174.
Lusher, A.L., McHugh, M., Thompson, R.C., 2013. Occurrence of microplastics in the gastrointestinal tract of pelagic and demersal fish from the English Channel. Mar. Pollut. Bull. 67, 94–99.
Meng, P.J., et al., 2009. Aquatic organotin pollution in Taiwan. J. Environ. Manag. 90 (Suppl 1), S8–15.
Merlo, E., Silva, I.V., Cardoso, R.C., Graceli, J.B., 2018. The obesogen tributyltin induces features of polycystic ovary syndrome (PCOS): a review. J. Toxicol. Environ. Health B Crit. Rev. 21, 181–206.
Mitra, S., Gera, R., Singh, V., Khandelwal, S., 2014. Comparative toxicity of low dose tributyltin chloride on serum, liver, lung and kidney following subchronic exposure. Food Chem. Toxicol. 64, 335–343.
Molinero, N., Ruiz, L., Sánchez, B., Margolles, A., Delgado, S., 2019. Intestinal bacteria interplay with bile and cholesterol metabolism: implications on host physiology. Front. Physiol. 10, 185.
Nowak, K., Jabłońska, E., Ratajczak-Wrona, W., 2019. Immunomodulatory effects of synthetic endocrine disrupting chemicals on the development and functions of human immune cells. Environ. Int. 125, 350–364.
Patterson, A.M., Mulder, I.E., Travis, A.J., Lan, A., Cerf-Bensussan, N., Gaboriau-Routhiau, V., Garden, K., Logan, E., Delday, M.I., Coutts, A., Monnais, E., Ferraria, V. C., Inoue, R., Grant, G., Aminov, R.I., 2017. Human gut symbiont roseburia hominis promotes and regulates innate immunity. Front. Immunol. 8, 1166.
Peeken, I., Primpke, S., Beyer, B., Gütermann, J., Katlein, C., Krumpen, T., Bergmann, M., Hehemann, L., Gerdts, G., 2018. Arctic sea ice is an important temporal sink and means of transport for microplastic. Nat. Commun. 9, 1505.
Qasem, W., Azad, M.B., Hossain, Z., Azad, E., Jorgensen, S., Castillo San Juan, S., Cai, C., Khafipour, E., Beta, T., Roberts, L.J., Friel, J., 2017. Assessment of complementary feeding of Canadian infants: effects on microbiome & oxidative stress, a randomized controlled trial. BMC Pediatr. 17, 54.
Rahmati, E., Martin, V., Wong, D., Sattler, F., Petterson, J., Ward, P., Butler-Wu, S.M., She, R.C., 2017. Facklamia species as an underrecognized pathogen. Open Forum Infect. Dis. 4, 272.
Rainieri, S., Conlledo, N., Larsen, B.K., Granby, K., Barranco, A., 2018. Combined effects of microplastics and chemical contaminants on the organ toxicity of zebrafish (Danio rerio). Environ. Res. 162, 135–143.
Rantakokko, P., Kuningas, T., Saastamoinen, K., Vartiainen, T., 2006. Dietary intake of organotin compounds in Finland: a market-basket study. Food Addit. Contam. 23, 749–756.
Redondo-Hasselerharm, P.E., Falahudin, D., Peeters, E., Koelmans, A.A., 2018. Microplastic effect thresholds for freshwater benthic macroinvertebrates. Environ. Sci. Technol. 52, 2278–2286.
Romeo, T., D'Alessandro, M., Esposito, V., Scotti, G., Berto, D., Formalewicz, M., Noventa, S., Giuliani, S., Macchia, S., Sartori, D., Mazzola, A., Andaloro, F., Giacobbe, S., Deidun, A., Renzi, M., 2015. Environmental quality assessment of Grand Harbour (Valletta, Maltese Islands): a case study of a busy harbour in the Central Mediterranean Sea. Environ. Monit. Assess. 187, 747.
Romo-Vaquero, M., Cortés-Martín, A., Loria-Kohen, V., Ramírez-de-Molina, A., García-Mantrana, I., Collado, M.C., Espín, J.C., Selma, M.V., 2019. Deciphering the human gut microbiome of urolithin metabotypes: association with enterotypes and potential cardiometabolic health implications. Mol. Nutr. Food Res. 63, 1800958.
de Sá, L.C., Oliveira, M., Ribeiro, F., Rocha, T.L., Futter, M.N., 2018. Studies of the effects of microplastics on aquatic organisms: what do we know and where should we focus our efforts in the future? Sci. Total Environ. 645, 1029–1039.
Schwabl, P., Köppel, S., Königshofer, P., Bucsics, T., Trauner, M., Reiberger, T., Liebmann, B., 2019. Detection of various microplastics in human stool: a prospective case series. Ann. Intern. Med. 171, 453–457.
Smith, M., Love, D.C., Rochman, C.M., Neff, R.A., 2018. Microplastics in seafood and the implications for human health. Curr. Environ. Health Rep. 5, 375–386.
Sokol, H., Pigneur, B., Watterlot, L., Lakhdari, O., Bermúdez-Humarán, L.G., Gratadoux, J.J., Blugeon, S., Bridonneau, C., Furet, J.P., Corthier, G., Grangette, C., Vasquez, N., Pochart, P., Trugnan, G., Thomas, G., Blottière, H.M., Doré, J., Marteau, P., Seksik, P., Langella, P., 2008. Faecalibacterium prausnitzii is an anti-inflammatory commensal bacterium identified by gut microbiota analysis of Crohn disease patients. Proc. Natl. Acad. Sci. USA 105, 16731–16736.
Sussarellu, R., Suquet, M., Thomas, Y., Lambert, C., Fabioux, C., Pernet, M.E., Le Goïc, N., Quillien, V., Mingant, C., Epelboin, Y., Corporeau, C., Guyomarch, J., Robbens, J., Paul-Pont, I., Soudant, P., Huvet, A., 2016. Oyster reproduction is affected by exposure to polystyrene microplastics. Proc. Natl. Acad. Sci. USA 113, 2430–2435.
Tahri, K., Grill, J.P., Schneider, F., 1997. Involvement of trihydroxyconjugated bile salts in cholesterol assimilation by bifidobacteria. Curr. Microbiol. 34, 79–84.
Tourinho, P.S., Kočí, V., Loureiro, S., van Gestel, C., 2019. Partitioning of chemical contaminants to microplastics: sorption mechanisms, environmental distribution and effects on toxicity and bioaccumulation. Environ. Pollut. 252, 1246–1256.
van Wezel, A., Caris, I., Kools, S.A., 2016. Release of primary microplastics from consumer products to wastewater in the Netherlands. Environ. Toxicol. Chem. 35, 1627–1631.
Wagner, M., Scherer, C., Alvarez-Muñoz, D., Brennholt, N., Bourrain, X., Buchinger, S., Fries, E., Grosbois, C., Klasmeier, J., Marti, T., Rodriguez-Mozaz, S., Urbatzka, R., Vethaak, A.D., Winther-Nielsen, M., Reifferscheid, G., 2014. Microplastics in freshwater ecosystems: what we know and what we need to know. Environ. Sci. Eur. 26, 12.
Wang, J., Ji, H., Wang, S., Liu, H., Zhang, W., Zhang, D., Wang, Y., 2018. Probiotic Lactobacillus plantarum promotes intestinal barrier function by strengthening the epithelium and modulating gut microbiota. Front. Microbiol. 9, 1953.
Wang, J., Liu, X., Li, Y., Powell, T., Wang, X., Wang, G., Zhang, P., 2019. Microplastics as contaminants in the soil environment: a mini-review. Sci. Total Environ. 691, 848–857.
Wexler, H.M., 2007. Bacteroides: the good, the bad, and the nitty-gritty. Clin. Microbiol. Rev. 20, 593–621.
Zhang, Z., Wu, X., Cao, S., Wang, L., Wang, D., Yang, H., Feng, Y., Wang, S., Li, L., 2016. Caffeic acid ameliorates colitis in association with increased Akkermansia population in the gut microbiota of mice. Oncotarget 7, 31790–31799.
Ziccardi, L.M., Edgington, A., Hentz, K., Kulacki, K.J., Kane Driscoll, S., 2016. Microplastics as vectors for bioaccumulation of hydrophobic organic chemicals in the marine environment: a state-of-the-science review. Environ. Toxicol. Chem. 35, 1667–1676.
Zollner, G., Trauner, M., 2008. Mechanisms of cholestasis. Clin. Liver Dis. 12, 1–26.